arXiv:1011.6531v1 [hep-ph] 30 Nov 2010

LU TP 10-27
November 2010

Vector Formfactors in Hard Pion Chiral Perturbation Theory

Johan Bijnens and Ilaria Jemos

Department of Astronomy and Theoretical Physics, Lund University,
Sölvegatan 14A, SE 223-62 Lund, Sweden

Abstract

We use three-flavour hard pion Chiral Perturbation Theory (HPChPT) in both the heavy meson and a relativistic formulation to calculate the chiral logarithms $m^2 \log\left(m^2/\mu^2\right)$ contributing to the formfactors of the $B_{(s)} \to \pi, K, \eta$ and $D_{(s)} \to \pi, K, \eta$ transitions at momentum transfer q^2 away from the endpoint $q^2_{\rm max} = (m_B - m_M)^2$. We compare our results with CLEO $D \to \pi$ and $D \to K$ data. We also calculate the Isgur-Wise function of the $B_{(s)} \to D_{(s)}$ semileptonic decay away from the endpoint and the chiral logarithms for the pion and kaon electromagnetic formfactor.

In two-flavour HPChPT we calculate the chiral logarithms for the pion vector and the scalar formfactors at $s \gg m_\pi^2$. This allows us to test hard pion ChPT using the existing two-loop calculations for these quantities.

PACS: 12.39.Fe Chiral Lagrangians, 13.20.He Decays of bottom mesons, 13.20.Fc Decays of charmed mesons, 11.30.Rd Chiral symmetries
Keywords: B and D meson semileptonic decays, Chiral Perturbation Theory

1 Introduction

As a result of the rapid progress in computer technology, simulations of full QCD on the lattice are becoming increasingly feasible and thus many results are now available. To improve their precision it is important to acquire control on all the sources of systematic errors involved. One of them is due to the fact that most simulations are done with meson masses larger then the physical ones. It is therefore essential to perform a chiral extrapolation of the lattice data points to achieve smaller meson masses.

In this respect Chiral Perturbation Theory (ChPT) [1, 2, 3], the effective field theory of QCD at low energy, plays a key role. This theory can predict the dependence on the light quark masses of the observables under study, via a systematic expansion in the masses and momenta of the light mesons using both the spontaneous and explicit breaking of chiral symmetry. Unfortunately ChPT is often limited by its range of validity. There exist several processes where it is applicable only in a small fraction of the allowed range of energy, while the extrapolations formulas are needed elsewhere. It is the case for example of the $K \to \pi$, $D \to \pi, K, \eta$ and $B \to \pi, K, \eta$ transition formfactors in e.g. semileptonic decays. These processes are very important for the determination of CKM matrix elements, obtained combining knowledge on the amplitudes from experiments [4, 5, 6, 7] and the formfactors calculated on the lattice [8]. The matching between lattice and experimental data is done when the momentum transfer squared to the vector boson is small, i.e. when a hard external pion arises and thus the power counting scheme of ChPT breaks down. However it is possible to exploit the chiral symmetry of QCD even there and predict the dependence on the meson masses of the formfactors using the arguments of hard pion Chiral Perturbation Theory (HPChPT).

This was first studied in [9] where it was applied to the semileptonic decay $K \to \pi$ using two-flavour ChPT. They argued there that it is possible to calculate the corrections of the type $m_\pi^2 \log m_\pi^2/\mu^2$ even when the squared momentum transfer q^2 is very small, i.e. when the outgoing pion is hard. Their arguments are based on the fact that only the soft internal pions are responsible for the chiral logarithms. These ideas have then been generalized and applied to $K \to \pi\pi$ [10] and to $B \to \pi\ell\nu_\ell$ [11], always in the framework of two-flavour ChPT. In [10, 11] it was made clear that the underlying arguments correspond basically to separate the hard-structure of a Feynman diagram from the soft one and use this last one to calculate infrared singularities. The arguments are essentially the same as those used for photon infrared singularities.

In this paper we use two-flavour HPChPT for the vector and the scalar formfactors of the pion $F_V^\pi(s)$ and $F_S^\pi(s)$ at $s \gg m_\pi^2$. Our main interest in this calculation is that it allows a test of the arguments of HPChPT using the existing two-loop results in standard two-flavour ChPT [12]. For completeness we also quote the three-flavour HPChPT results for the electromagnetic formfactor for pions and kaons.

The main new result of this work is the three-flavour HPChPT calculation of the transition formfactors in vector transitions of B and D to π, K and η and the Isgur-Wise function in B to D transitions. In the latter case, the calculations did exist and has been used but the validity of the formulas was not discussed. Our results improve

the comparison between the measured $D \to \pi$ and $D \to K$ formfactors [4]. We also calculate the contributions at the endpoint for all these transitions where the results for the transitions to η are new.

The paper is organized as follows. In Sect. 2 we briefly review ChPT and heavy meson ChPT (HMChPT). We present the relativistic theory that has been used to have an extra check of the correctness of our results here as well. At the end of this section we also summarize the arguments why HPChPT works, although we refer the reader for further details to Sect. 5 of [11].

In Sect. 3 we present the results for pion and kaon formfactors and test HPChPT using the existing two-flavour two-loop calculations for the pion formfactors. In Sect. 4 we define the formfactors of the heavy to light transitions and present our results for them. We also show here the comparison with the experimental data from [4] on the $D \to \pi(K)$ transitions . The $B \to D$ transitions are defined and our results for them given in Sect. 5. In the appendix we provide some results for the needed expansions of the loop integrals.

2 Chiral Perturbation Theory

2.1 Standard Chiral Perturbation Theory

In this subsection we briefly describe the formalism of ChPT [1, 2, 3] for both two- and three-flavour ChPT. The notation in the following is the same as in [13]. The lowest order Lagrangian describing the strong interactions of the light mesons is

$$\mathcal{L}^{(2)}_{\pi\pi} = \frac{F^2}{4}\left(\langle u_\mu u^\mu\rangle + \langle \chi_+\rangle\right), \tag{1}$$

with

$$\begin{aligned} u_\mu &= i\{u^\dagger(\partial_\mu - ir_\mu)u - u(\partial_\mu - il_\mu)u^\dagger\}\,, \\ \chi_\pm &= u^\dagger\chi u^\dagger \pm u\chi^\dagger u\,, \\ u &= \exp\left(\frac{i}{\sqrt{2}F}\phi\right)\,, \\ \chi &= 2B(s+ip)\,. \end{aligned}$$

u parametrizes the oscillations around the vacuum in $SU(n)_L \times SU(n)_R/SU(n)_V \sim SU(n)$ for $n = 2, 3$ the number of light flavours. ϕ is thus a hermitian $n \times n$ matrix:

$$\phi = \begin{pmatrix} \frac{1}{\sqrt{2}}\pi^0 + \frac{1}{\sqrt{6}}\eta & \pi^+ & K^+ \\ \pi^- & -\frac{1}{\sqrt{2}}\pi^0 + \frac{1}{\sqrt{6}}\eta & K^0 \\ K^- & \bar{K}^0 & -\frac{2}{\sqrt{6}}\eta \end{pmatrix}, \qquad \phi = \begin{pmatrix} \frac{1}{\sqrt{2}}\pi^0 & \pi^+ \\ \pi^- & -\frac{1}{\sqrt{2}}\pi^0 \end{pmatrix}. \tag{2}$$

The fields s, p, $l_\mu = v_\mu - a_\mu$ and $r_\mu = v_\mu + a_\mu$ are the standard external scalar, pseudoscalar, left- and right-handed vector fields introduced by Gasser and Leutwyler [2, 3]. We will use

the symbol F throughout this paper but it should be kept in mind that F can be either the two-flavour constant called F in [2] or the three-flavour one called F_0 in [3].

The field u and u_μ transform under a chiral transformation $g_L \times g_R \in SU(n)_L \times SU(n)_R$ as

$$u \longrightarrow g_R u h^\dagger = h u g_L^\dagger, \qquad u_\mu \longrightarrow h u_\mu h^\dagger. \tag{3}$$

In (3) h depends on u, g_L and g_R and is the so called compensator field. The notation $\langle X \rangle$ stands for trace over up,down quark indices for $n = 2$ and up, down, strange for $n = 3$.

Starting from this Lagrangian we can then build an effective field theory by including loop diagrams and higher order Lagrangians. Introductions to ChPT can be found in [14, 15].

2.2 Heavy meson Chiral Perturbation Theory

In this subsection we briefly describe the formalism of HMChPT [16, 17, 18]. Longer introductions can be found in the lectures by Wise [19] and the book [20].

The combination of Heavy Quark Effective Theory and of ChPT provides us with a powerful formalism to study hadrons containing a heavy quark. This combination is called HMChPT. It makes use of both spontaneously broken $SU(n)_L \times SU(n)_R$ chiral symmetry on the light quarks, and spin-flavour symmetry on the heavy quarks. Thus HMChPT involves both a heavy and a light scale. The first one is the heavy meson mass and rules an expansion in powers of its inverse. The second is the light meson mass that lets us study chiral symmetry breaking effects in a chiral-loop fashion as in standard ChPT.

The sector of the Lagrangian involving only light-quarks has already been discussed above. We now present the heavy meson part of the HMChPT Lagrangian for the three-flavour case [16, 17, 18]. Hereafter we concentrate on the $B^{(*)}$ mesons, but the same equations hold for the $D^{(*)}$ mesons as well. In the limit $m_b \to \infty$, the pseudoscalar, B, and the vector, B^*, mesons are degenerate. All results in this paper are in the leading order in the heavy quark expansion. Thus in the following we neglect the mass splitting $\Delta = m_{B^*} - m_B$. To implement the heavy quark symmetries it is convenient to assemble them into a single field

$$H_a(v) \;=\; \frac{1+\not{v}}{2}\left[B^*_{a\mu}(v)\gamma^\mu - B_a(v)\gamma_5\right], \tag{4}$$

where v is the fixed four-velocity of the heavy meson, a is a flavour index corresponding to the light quark in the heavy meson. Therefore $B_1 = B^+$, $B_2 = B^0$, $B_3 = B_s$, while $D_1 = \overline{D^0}$, $D_2 = D^-$, $D_3 = \overline{D_s}$ and similarly for the vector mesons B^*_μ and D^*_μ. In (4) the operator $(1+\not{v})/2$ projects out the particle component of the heavy meson only. The conjugate field is defined as $\overline{H}_a(v) \equiv \gamma_0 H_a^\dagger(v)\gamma_0$. We assume the field $H_a(v)$ to transform under the chiral transformation $g_L \times g_R \in SU(n)_L \times SU(n)_R$ as

$$H_a(v) \longrightarrow h_{ab} H_b(v)\,, \tag{5}$$

so we introduce the covariant derivative

$$D^{\mu}_{ab} H_b(v) = \delta_{ab} \partial^{\mu} H_b(v) + \Gamma^{\mu}_{ab} H_b(v), \tag{6}$$

where $\Gamma^{\mu}_{ab} = \frac{1}{2}\left[u^{\dagger}\left(\partial_{\mu} - i r_{\mu}\right) u + u\left(\partial_{\mu} - i l_{\mu}\right) u^{\dagger}\right]_{ab}$, and the indices a, b run over the light quark flavours. Finally, the Lagrangian for the heavy-light mesons in the static heavy quark limit reads

$$\mathcal{L}_{\text{heavy}} = -i \,\text{Tr}\left[\overline{H}_a v \cdot D_{ab} H_b\right] + g \,\text{Tr}\left[\overline{H}_a u^{\mu}_{ab} H_b \gamma_{\mu} \gamma_5\right], \tag{7}$$

where g is the coupling of the heavy meson doublet to the Goldstone boson and the traces, Tr, are over spin indices, the γ-matrix indices. The Lagrangian (7) satisfies chiral symmetry and heavy quark spin flavour symmetry. We neglect in the following the mass differences for the heavy mesons containing the same heavy quark.

2.3 Relativistic theory

When the momentum transfer to the light degrees of freedom is not small as in HPChPT, very off-shell heavy mesons may appear in the loops. Different treatments of the off-shell behaviour modify the loop-functions. Thus in principle it might change the non-analyticities in the light meson masses. If this were the case, the arguments summarized in Sect. 2.4 would be wrong. In fact, provided that the two formalisms are both sufficiently complete, the soft singularities must be the same, since they are arising in the same way. This is the reason why both here and in [11] we are calculating not only using HMChPT but also in a relativistic formulation as a check on the arguments.

We use a relativistic Lagrangian that respects the spin-flavour symmetries of HMChPT. It is essentially the same Lagrangian introduced in [11], but now in the three-flavour case. The B_a and $B^*_{a\mu}$ fields are in the relativistic form and we treat them as column-vectors in the light-flavour index a.

$$\begin{aligned}
\mathcal{L}_{\text{kin}} &= \nabla^{\mu} B^{\dagger} \nabla_{\mu} B - m_B^2 B^{\dagger} B - \frac{1}{2} B^{*\dagger}_{\mu\nu} B^{*\mu\nu} + m_B^2 B^{*\dagger}_{\mu} B^{*\mu}, &(8)\\
\mathcal{L}_{\text{int}} &= g M_0 \left(B^{\dagger} u^{\mu} B^*_{\mu} + B^{*\dagger}_{\mu} u^{\mu} B\right) \\
&+ \frac{g}{2} \epsilon^{\mu\nu\alpha\beta} \left(-B^{*\dagger}_{\mu} u_{\alpha} \nabla_{\mu} B^*_{\beta} + \nabla_{\mu} B^{*\dagger}_{\nu} u_{\alpha} B^*_{\beta}\right), &(9)
\end{aligned}$$

with $B^*_{\mu\nu} = \nabla_{\mu} B^*_{\nu} - \nabla_{\nu} B^*_{\mu}$, and $\nabla_{\mu} = \partial_{\mu} + \Gamma_{\mu}$. The constant g of (9) is the same in (7), M_0 is the mass of the B meson in the chiral limit. The fields B and B^* transform under chiral transformations as $B \to hB$. The two terms of $\mathcal{L}_{\text{int}}$ in (9) contain the vertices BB^*M and B^*B^*M for $M = \pi, K, \eta$.

From $\mathcal{L}_{\text{kin}}$ in (8) we find the propagators of the B and B^* meson respectively:

$$\frac{i}{p^2 - m_B^2}, \qquad \frac{-i\left(g_{\mu\nu} - \frac{p_{\mu} p_{\nu}}{m_B^2}\right)}{p^2 - m_B^2}. \tag{10}$$

This is to be contrasted with the propagator $1/v \cdot p$ in the HMChPT showing the different off-shell behavior.

2.4 Hard pion Chiral Perturbation Theory

In general, the use of ChPT and HMChPT is valid as long as the interacting light mesons are soft, i.e. if they have momenta much smaller than the scale of spontaneous chiral symmetry breaking ($\Lambda_{\rm ChSB} \simeq 1$ GeV). Only in this regime is the power counting of ChPT well defined.

On the other hand the arguments presented in great detail in Sect. 5 of [11] show that the predictions of the soft singularities in the light meson masses appearing in the final amplitudes are reliable even outside the range of applicability of HMChPT. Hereafter we present a short summary of these arguments, but for a comprehensive discussion we refer the reader to Sect. 5 of [11].

The underlying idea is that in a loop diagram, the internal soft light mesons are the source of the infrared non-analyticities arising, even if hard, i.e. large momentum, light mesons are present. Since the soft lines do not see the hard or short-distance structure of the diagram, we can separate them from the rest of the process. We should thus be able to describe the hard part of any diagram by an effective Lagrangian which must include the most general terms consistent with all the symmetries. The coefficients of this Lagrangian depend on the hard kinematical quantities and can even be complex. This Lagrangian must be sufficiently complete to describe the neighbourhood of the underlying hard process.

Extra caution must be taken to build up the Lagrangian describing the hard part. As a matter of fact we can not neglect operators with an arbitrary numbers of derivatives since the momenta into play can be large. However it turns out that matrix elements of operators with higher number of derivatives are all proportional to the lowest order ones up to terms of higher order, i.e. the coefficients of the leading non-analyticities are calculable in terms of the lowest order Lagrangians.

We expect that a full power counting can be formulated along the lines of SCET [21] but the leading prediction can be obtained in the simpler fashion done here.

3 Pion and kaon formfactors

3.1 Electromagnetic formfactors in three-flavour HPChPT

The vector (electromagnetic) formfactors of the charged pion and kaon are defined as

$$\left\langle \pi(K)^+(p_2) \left| j_\mu^{\rm elm} \right| \pi(K)^+(p_1) \right\rangle \;=\; (p_2+p_1)_\mu F_V^{\pi(K)}(s), \tag{11}$$

with $s=(p_1-p_2)^2$ and $j_\mu^{\rm elm} = \frac{2}{3}\bar{u}\gamma_\mu u - \frac{1}{3}\bar{d}\gamma_\mu d - \frac{1}{3}\bar{s}\gamma_\mu s$ is the electromagnetic current. The arguments of HPChPT can be used here as well and we get from the relevant one-loop diagrams and wave function renormalization that

$$\begin{aligned} F_V^\pi(s) &= F_V^{\pi\chi}(s)\left(1+\frac{1}{F^2}\overline{A}(m_\pi^2)+\frac{1}{2F^2}\overline{A}(m_K^2)+\mathcal{O}(m_L^2)\right), \\ F_V^K(s) &= F_V^{K\chi}(s)\left(1+\frac{1}{2F^2}\overline{A}(m_\pi^2)+\frac{1}{F^2}\overline{A}(m_K^2)+\mathcal{O}(m_L^2)\right). \end{aligned} \tag{12}$$

The superscript χ here means in the limit $m_u = m_d = m_s = 0$. In the remainder we will usually drop the $\mathcal{O}(m_L^2)$ part but all results should be interpreted as up to analytic terms in the light meson masses squared. The loop integral $\overline{A}(m^2)$ is defined in the appendix. The result (12) can be calculated directly or by expanding the known ChPT result [22, 23] for $s \gg m_L^2$.

3.2 Vector and scalar pion formfactors in two-flavour HPChPT

It is important to test the arguments behind HPChPT as much as possible. We can do a nontrivial test by looking at the two-flavour case for the pion vector and scalar formfactors. The vector form factor is defined in (11) and the scalar formfactor is defined by

$$\left\langle \pi^0(p_2) \left| \bar{u}u + \bar{d}d \right| \pi^0(p_1) \right\rangle \quad = \quad f_S^\pi(0) F_S^\pi(s) \,. \tag{13}$$

We have factored out here as is customary [2, 22, 12] the value at $s = 0$. From the general discussion we again expect that the leading non-analytic correction should be in both cases of the form

$$f(s) = C(s) \times \left(1 + \alpha \frac{m^2}{F^2} \log \frac{m^2}{\mu^2} + \mathcal{O}(m^2) \right) . \tag{14}$$

In principle α could depend on s but it is calculable. $C(s)$ is a free parameter in HPChPT and can even be complex.

Calculating the formfactors from wave-function renormalization and the needed one-loop diagrams we obtain

$$\begin{aligned} F_V^\pi(s) &= F_V^{\pi\chi}(s) \left(1 + \frac{1}{F^2} \overline{A}(m_\pi^2) \right) , \\ F_S^\pi(s) &= F_S^{\pi\chi}(s) \left(1 + \frac{5}{2F^2} \overline{A}(m_\pi^2) \right) . \end{aligned} \tag{15}$$

Here χ means in the limit $m_u = m_d = 0$. This agrees with the large s expansion of the one-loop result of [2].

In normal ChPT these formfactors are known fully analytically up till two-loop order [12]. We can now choose a value of m_π^2 and s such that $s \gg m_\pi^2$ but with both s and m_π^2 in the regime of validity of standard HPChPT. The expansion for $s \gg m_\pi^2$ can be done and the result should be of the form (15) where the form of $F_V^{\pi\chi}(s)$, $F_S^{\pi\chi}(s)$ follows from the one-loop calculation in the limit $m_\pi^2 = 0$. This gives

$$\begin{aligned} F_V^{\pi\chi}(s) &= 1 + \frac{s}{16\pi^2 F^2} \left(\frac{5}{18} - 16\pi^2 l_6^r + \frac{i\pi}{6} - \frac{1}{6} \ln \frac{s}{\mu^2} \right) , \\ F_S^{\pi\chi}(s) &= 1 + \frac{s}{16\pi^2 F^2} \left(1 + 16\pi^2 l_4^r + i\pi - \ln \frac{s}{\mu^2} \right) . \end{aligned} \tag{16}$$

Let us see what happens when the full two-loop results are taken into account. Our arguments still hold as long as we are working at the desired order i.e. $\mathcal{O}(m_\pi^2)$. On the

other hand now different kind of terms arise. Some of them are suppressed by m_π^4 with or without logarithms and so can be neglected. The ones like s^2 or $s^2 \log s^2/\mu^2$ and without $\log(m_\pi^2/\mu^2)$ cannot be predicted by HPChPT and are absorbed in the unknown part of the coefficient $C(s)$ of (14). Terms like $s^2 \log^2 m_\pi^2/\mu^2$ or $s^2 \log m_\pi^2/\mu^2$ can also arise. Those not only would be large in our limit, but even divergent when $m_\pi \to 0$, therefore they must cancel. Terms like $s m_\pi^2 \log^2 m_\pi^2/\mu^2$ are predicted by HPChPT not to occur. Finally there are terms as $s m_\pi^2 \log(m_\pi^2/\mu^2)$ and $s m_\pi^2 \log(m_\pi^2/\mu^2) \log(s/\mu^2)$ which are of special interest. The coefficients of these are predicted by HPChPT. They are given by (16) and (15). Performing the expansion of the full two-loop result for $s \gg m_\pi^2$ we indeed find that the result is of the required form with the chiral limit value given exactly by (16). This is a rather nontrivial check on HPChPT.

4 $B \to M$ and $D \to M$ transitions

4.1 Definition of formfactors

In this section we review the formalism for the transitions of a B or a D meson into a light pseudoscalar meson (π, K, η). We restrict ourselves to the case of a B meson, but the same definitions hold also for the D-decay. All the following discussion can be found also in [11] for the two-flavour case. We report it here for the sake of completeness. The hadronic current for pseudoscalar to pseudoscalar vector transitions ($P_i(\bar{q}_i, q) \to P_f(\bar{q_f}, q)$) has the structure

$$\begin{aligned} \langle P_f(p_f) \left| \overline{q}_i \gamma_\mu q_f \right| P_i(p_i) \rangle &= (p_i + p_f)_\mu f_+(q^2) + (p_i - p_f)_\mu f_-(q^2) \\ &= \left[(p_i + p_f)_\mu - q_\mu \frac{(m_i^2 - m_f^2)}{q^2} \right] f_+(q^2) + q_\mu \frac{(m_i^2 - m_f^2)}{q^2} f_0(q^2), \end{aligned} \tag{17}$$

where q^μ is the momentum transfer $q^\mu = p_i^\mu - p_f^\mu$. In our case P_f is a light pseudoscalar meson, P_i is a B meson and $q_i = b$. For example, to find the $B^0 \to \pi^+$ formfactors we need then to evaluate the hadron matrix elements of the quark bilinear $\overline{b}\gamma_\mu q$, where $q = u$.

Parity invariance, heavy quark and chiral symmetry dictate that the matching of QCD bilinears onto operators of HMChPT take the form [24, 19],

$$\bar{b}\gamma^\mu q_a \propto c \left\{ \mathrm{Tr}\left[\gamma^\mu \left(u_{ab}^\dagger + u_{ab} \right) H_b(v) \right] + \mathrm{Tr}\left[\gamma_5 \gamma^\mu \left(u_{ab}^\dagger - u_{ab} \right) H_b(v) \right] \right\}. \tag{18}$$

If no hard pions appear in the final state we can use the definition of the decay constant

$$\left\langle 0 \left| \overline{b}\gamma_\mu \gamma_5 q \right| B(p_B) \right\rangle = i F_B p_B^\mu \tag{19}$$

and obtain $c = \frac{1}{2} F_B \sqrt{m_B}$. This latter result does not hold for momenta away from q^2_{max} in which case c is just an effective coupling depending on q^2.

In HMChPT the definitions of the formfactors are chosen such that those are independent of the heavy meson mass. So for example for the $B \to M$ transition

$$\left\langle M(p_M) \left| \overline{b}\gamma_\mu q \right| B(v) \right\rangle_{\mathrm{HMChPT}} = \left[p_{M\mu} - (v \cdot p_M)\, v_\mu \right] f_p(v \cdot p_M) + v_\mu f_v(v \cdot p_M). \tag{20}$$

In (20) $v \cdot p_M$ is the energy of the light meson in the heavy meson rest frame

$$v \cdot p_M = \frac{m_B^2 + m_M^2 - q^2}{2m_B}. \tag{21}$$

The formfactors defined in (17) and in (20) are related by matching the relativistic and the HMChPT hadronic current:

$$\begin{aligned} \sqrt{m_B} f_p(v \cdot p_M) &= f_+(q^2) + \frac{m_B^2 - m_M^2}{q^2} f_+(q^2) - \frac{m_B^2 - m_M^2}{q^2} f_0(q^2) \\ &= f_+(q^2) - f_-(q^2), \end{aligned} \tag{22}$$

$$\begin{aligned} \sqrt{m_B}\left(f_v(v \cdot p_M) - f_p(v \cdot p_M) v \cdot p_M\right) &= m_B \left(\frac{q^2 - m_B^2 + m_M^2}{q^2} f_+(q^2) + \frac{m_B^2 - m_M^2}{q^2} f_0(q^2) \right) \\ &= m_B \left(f_+(q^2) + f_-(q^2) \right). \end{aligned} \tag{23}$$

The $\sqrt{m_B}$ factors in (22) and (23) are due to the different normalizations of states used in the two formalisms. At $q^2 \approx q^2_{\rm max}$, neglecting terms suppressed by powers of m_M and of $1/m_B$, (22) and (23) become

$$f_0(q^2) = \frac{1}{\sqrt{m_B}} f_v(v \cdot p_M), \qquad f_+(q^2) = \frac{\sqrt{m_B}}{2} f_p(v \cdot p_M). \tag{24}$$

We remark that the relations in (24) are valid only when $q^2 \approx q^2_{\rm max}$ contrary to what was said in the original version[1] of [11]. At general q^2 away from $q^2_{\rm max}$ we must use (22) and (23).

A matching similar to (18) has to be done also for the relativistic theory described in Sect. 2.3. We identify four possible operators[2]

$$J^L_\mu = \frac{1}{2} E_1 t u^\dagger \nabla_\mu B + \frac{i}{2} E_2 t u^\dagger u_\mu B + \frac{i}{2} E_3 t u^\dagger B^*_\mu + \frac{1}{2} E_4 t u^\dagger \left(\nabla_\nu u_\mu\right) B^{*\nu}, \tag{25}$$

where E_1,..., E_4, are effective couplings. t is a constant spurion vector transforming as $t \to t g_L^\dagger$, so that J^L_μ is invariant under $SU(3)_L$ transformations. The heavy quark symmetry implies $m_B E_1 = E_3$. Analogously we can introduce a right-handed J^R_μ current and thus an axial-vector $J^5_\mu = J^R_\mu - J^L_\mu$ and a vector $J^V_\mu = J^R_\mu + J^L_\mu$ current. They are used respectively to evaluate the amplitudes of $B \to \ell \nu_\ell$ and the $B \to M$ formfactors as defined in (17). We leave the discussion for the latter in Sects. 4.2 and 4.4, while we quote here the expression of the $B(B_s)$ decay constants that can be found evaluating the $B(B_s) \to$ vacuum matrix element at one loop:

$$F_B = E_1 \left\{ 1 + \frac{1}{F^2} \left[\left(\frac{3}{8} + \frac{9}{8} g^2 \right) \overline{A}(m_\pi^2) + \left(\frac{1}{4} + \frac{3}{4} g^2 \right) \overline{A}(m_K^2) + \left(\frac{1}{24} + \frac{1}{8} g^2 \right) \overline{A}(m_\eta^2) \right] \right\},$$

[1] Notice that this does not invalidate the results of [11]. Indeed all the formfactors involved have the same chiral logarithms, thus the tree-level part can still be factorized out, as shown in Sect. 4.2

[2] The last one is higher order but we included it since it has a different type of contraction of the Lorentz indices and as an explicit check on the arguments of HPChPT [11].

Figure 1: The tree-level diagrams contributing to the amplitude. A double line corresponds to a B, a zigzag line to a B^*, a single line to a light meson, i.e. π, K or η. A black circle represents the insertion of a vector current.

$$F_{B_s} = E_1 \left\{ 1 + \frac{1}{F^2} \left[\left(\frac{1}{2} + \frac{3}{2} g^2 \right) \overline{A}(m_K^2) + \left(\frac{1}{6} + \frac{1}{2} g^2 \right) \overline{A}(m_\eta^2) \right] \right\}. \tag{26}$$

$$\tag{27}$$

$\overline{A}(m^2)$ is defined in (A.1) in the appendix. Here we only quote the non-analytic dependence on the light quark masses for the one-loop part. The results (26) and (27) agree with those obtained with HMChPT [18]. We see that E_1 plays the role of F_H in [18] and that the relativistic theory predicts the same coefficient of the chiral logarithm in $\overline{A}(m^2)$ as expected.

4.2 The chiral logarithms away from the endpoint

In this section we present results for the formfactors of the vector transitions $B \to \pi$, $B \to K$, $B \to \eta$, $B_s \to K$ and $B_s \to \eta$ calculated using three-flavour HPChPT. The results for the $B \to \pi$ transition in two-flavour ChPT can be found in [11]. We quote only the relevant terms, i.e. the leading ones which contain free parameters and the predicted chiral logarithms up to $\mathcal{O}(m_M^2)$. The tree-level diagrams contributing to the amplitude are shown in Fig. 1. The formfactors at tree level read for HMChPT

$$f_p^{\text{Tree}}(v \cdot p_M) = C_{B\to M} \frac{\alpha}{F} \frac{g}{v \cdot p_M + \Delta}, \qquad f_v^{\text{Tree}}(v \cdot p_M) = C_{B\to M} \frac{\alpha}{F}, \tag{28}$$

where $C_{B\to M}$ is a constant that changes depending on the meson transition and takes the values

$$C_{B\to M} = \begin{cases} 1 & B^- \to \pi^0 \\ \sqrt{2} & \bar{B}^0 \to \pi^+ \\ \sqrt{2} & B \to K \\ \frac{1}{\sqrt{3}} & B \to \eta \\ \sqrt{2} & B_s \to K \\ -\frac{2}{\sqrt{3}} & B_s \to \eta. \end{cases} \tag{29}$$

In (28) α is a constant that takes the value $\sqrt{m_B/2} F_B$ at q^2_{max}. We also obtain $c = \alpha/\sqrt{2}$. Near $q^2_{max} = (m_B - m_M)^2$ the results remain obviously the same, but the propagator in

the first equation of (28) becomes $1/m_M$. In the case of the relativistic theory of Sect. 2.3, we distinguish the formfactors for the two q^2 ranges. At q^2 away from $q^2_{\rm max}$

$$f_+^{\rm Tree}(q^2) = C_{B\to M}\left\{-\frac{1}{4}\frac{E_3}{F}\frac{m_B}{q^2-m_B^2}g+\frac{1}{8}\frac{E_1}{F}-\frac{1}{4}\frac{E_2}{F}\right\},$$
$$f_0^{\rm Tree}(q^2) = C_{B\to M}\left\{\frac{1}{8}\frac{E_1}{F}\left(1+\frac{q^2}{m_B^2-m_M^2}\right)-\frac{1}{4}\left(\frac{E_2}{F}+\frac{E_3}{F}\frac{m_B}{q^2-m_B^2}g\right)\left(1-\frac{q^2}{m_B^2-m_M^2}\right)\right\}. \tag{30}$$

At $q^2 \approx q^2_{\rm max}$ (30) simplifies to

$$f_+^{\rm Tree}(q^2)_{q^2\approx q^2_{\rm max}} = C_{B\to M}\frac{1}{4}\frac{E_3}{F}\frac{1}{2m_M}g, \qquad f_0^{\rm Tree}(q^2)_{q^2\approx q^2_{\rm max}} = C_{B\to M}\frac{1}{4}\frac{E_1}{F}. \tag{31}$$

We stress once more that the relation of E_1 and E_3 to F_B holds only when $q^2 \approx q^2_{max}$. As the momentum transfer is out of this range the coupling constant are different at the different values of q^2 and can even be complex.

At one-loop we need to include the contributions of the wavefunction renormalization Z_π, Z_K, Z_η, Z_B and Z_{B_s}. They are the same for HMChPT and the relativistic theory and read:

$$\begin{aligned}
Z_\pi &= 1-\frac{2}{3}\frac{\overline{A}(m_\pi^2)}{F^2}-\frac{1}{3}\frac{\overline{A}(m_K^2)}{F^2},\\
Z_K &= 1-\frac{1}{4}\frac{\overline{A}(m_\pi^2)}{F^2}-\frac{1}{2}\frac{\overline{A}(m_K^2)}{F^2}-\frac{1}{4}\frac{\overline{A}(m_\eta^2)}{F^2},\\
Z_\eta &= 1-\frac{\overline{A}(m_K^2)}{F^2},\\
Z_B &= 1+\frac{9}{4}g^2\frac{\overline{A}(m_\pi^2)}{F^2}+\frac{3}{2}g^2\frac{\overline{A}(m_K^2)}{F^2}+\frac{3}{12}g^2\frac{\overline{A}(m_\eta^2)}{F^2},\\
Z_{B_s} &= 1+3g^2\frac{\overline{A}(m_K^2)}{F^2}+g^2\frac{\overline{A}(m_\eta^2)}{F^2}.
\end{aligned} \tag{32}$$

The one-loop corrections to the vector current J_μ^V are shown in Fig. 2.

To find the results in HMChPT we expanded the one-loop calculation of [25] at $v\cdot p_M \to m_B$, $m_M^2 \to 0$. Note however that their results are only valid near the endpoint. The arguments of HPChPT allow us to use their results also away from the endpoint.

In the relativistic theory we first calculated the formfactors and then we expanded the loop integrals for $m_M^2 \ll m_B^2, (m_B^2-q^2)$. These latter expansions are given in App. A. Notice that we keep terms of the kind m/M in the expansion of the $\bar{C}$ and $\bar{B}$ functions (A.8), (A.9) that had not been included explicitly in [11]. Those terms could cause corrections like mM/F^2 in the final results, that would violate the heavy quark limit $M\to\infty$. We verified that all these corrections do cancel. To achieve the final results, we sum up all the contributions coming from the several diagrams and include the wavefunction renormalization pieces. This corresponds to sum $(1/2)Z_M$ for $M=\pi,K,\eta$ and $(1/2)Z_B$ or $(1/2)Z_{B_s}$,

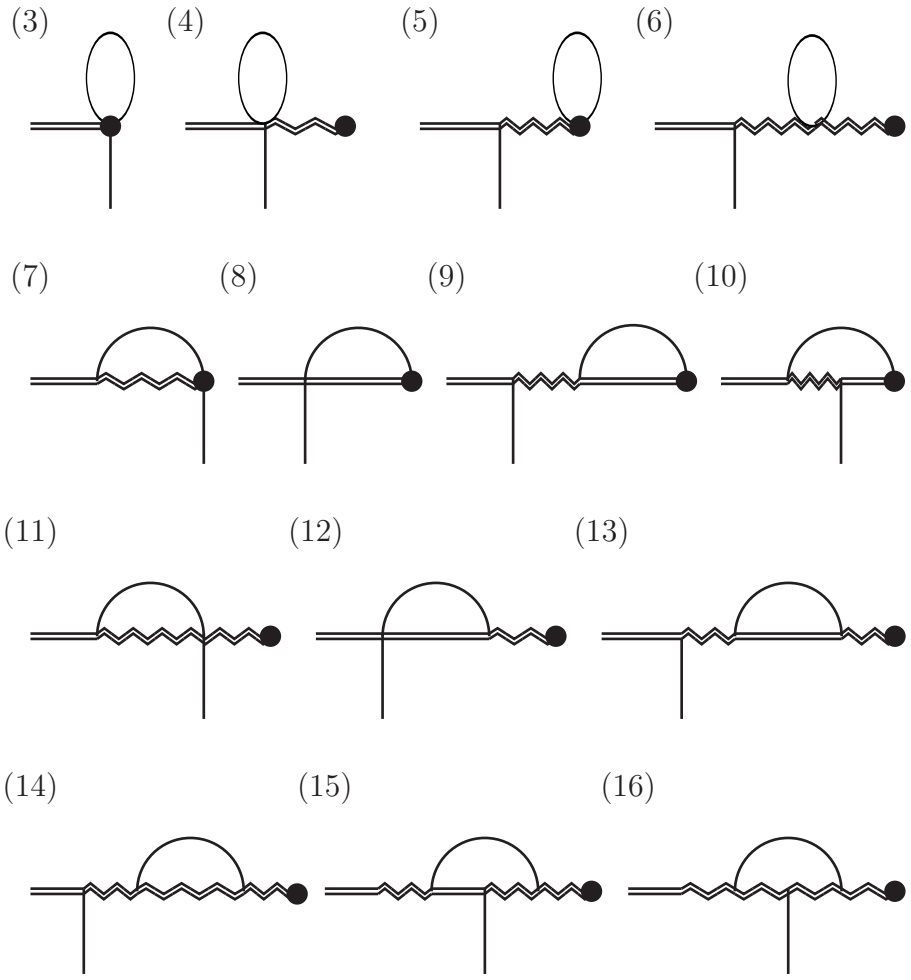

Figure 2: The one-loop diagrams contributing to the amplitude. Vertices and lines as in Fig. 1

according to the external legs of the process under study, multiplied by the tree-level part of the formfactors. We find for the different transitions that the two formfactors always have the same chiral logarithms. We can write the results in the form

$$f_{v/p}(v \cdot p_M) = f_{v/p}^{\rm Tree}(v \cdot p_M) F_{B\to M} \tag{33}$$

The chiral logarithms are in $F_{B\to M}$ and read for the different transitions

$$\begin{aligned} F_{B\to\pi} &= 1 + \left(\frac{3}{8} + \frac{9}{8}g^2\right)\frac{\overline{A}(m_\pi^2)}{F^2} + \left(\frac{1}{4} + \frac{3}{4}g^2\right)\frac{\overline{A}(m_K^2)}{F^2} + \left(\frac{1}{24} + \frac{1}{8}g^2\right)\frac{\overline{A}(m_\eta^2)}{F^2}, \\ F_{B\to K} &= 1 + \frac{9}{8}g^2\frac{\overline{A}(m_\pi^2)}{F^2} + \left(\frac{1}{2} + \frac{3}{4}g^2\right)\frac{\overline{A}(m_K^2)}{F^2} + \left(\frac{1}{6} + \frac{1}{8}g^2\right)\frac{\overline{A}(m_\eta^2)}{F^2}, \end{aligned}$$

$$
\begin{aligned}
F_{B\to\eta} &= 1+\left(\frac{3}{8}+\frac{9}{8}g^2\right)\frac{\overline{A}(m_\pi^2)}{F^2}+\left(\frac{1}{4}+\frac{3}{4}g^2\right)\frac{\overline{A}(m_K^2)}{F^2}+\left(\frac{1}{24}+\frac{1}{8}g^2\right)\frac{\overline{A}(m_\eta^2)}{F^2}\,,\\
F_{B_s\to K} &= 1+\frac{3}{8}\frac{\overline{A}(m_\pi^2)}{F^2}+\left(\frac{1}{4}+\frac{3}{2}g^2\right)\frac{\overline{A}(m_K^2)}{F^2}+\left(\frac{1}{24}+\frac{1}{2}g^2\right)\frac{\overline{A}(m_\eta^2)}{F^2}\,,\\
F_{B_s\to\eta} &= 1+\left(\frac{1}{2}+\frac{3}{2}g^2\right)\frac{\overline{A}(m_K^2)}{F^2}+\left(\frac{1}{6}+\frac{1}{2}g^2\right)\frac{\overline{A}(m_\eta^2)}{F^2}\,.
\end{aligned}
\tag{34}
$$

$F_{B_s\to\pi}$ vanishes due to the possible flavour quantum numbers.

In all the transitions we obtain, as predicted by our arguments, the same coefficients for the relativistic theory. I.e.

$$
f_{+/0}(q^2)=f_{+/0}^{\rm Tree}(q^2)F_{B\to M}\,. \tag{35}
$$

The correction is also the same for the formfactors f_0 and f_+ or for f_v and f_p in all the cases. Notice that (34) is also in agreement with the results in two-flavour HPChPT of [11]

The chiral logarithms for both form factors are always the same in these decays as can be seen in (35) and (33). This was also already the case for the $K_{\ell 3}$ formfactors in HPChPT [9] and we noticed it as well in [11]. It cannot simply be something like heavy quark symmetry since it is not valid at the endpoint, see below and [24, 25]. This would also not be a valid reason for the $K_{\ell 3}$ case. An alternative explanation would be if something similar to Low's theorem for electromagnetic soft corrections holds. Low's theorem states that the amplitude for the process with Bremsstrahlung is proportional to the amplitude without Bremsstrahlung by a factor depending only on the external legs. A corresponding result holds for the infrared logarithms in virtual photon diagrams. But, if here there was only dependence on the external legs, we obtain the relation

$$
F_{B\to K}-F_{B\to\eta}-F_{B_s\to K}+F_{B_s\to\eta}=0\,. \tag{36}
$$

Inspection of the results in (34) show that this is not satisfied. The same argument would have predicted that the chiral logarithms in $F_V^\pi(s)$ and $F_S^\pi(s)$ of (15) are the same which is again clearly not the case.

4.3 Comparison with experiment

We did not find any lattice data published in a form that allows us to test the chiral logarithms in (34). However, there are published data on the formfactors in $D\to\pi$ and $D\to K$ semileptonic decays. The most precise data come from CLEO. In [4] are reported the data points of $f_+(q^2)|V_{cd}|$ for $D^{+(0)}\to\pi^{0(+)}$ decays and of $f_+(q^2)|V_{cs}|$ for $D^{0(+)}\to K^{+(0)}$ decays. We can then use the known value for the Cabibbo angle to get at the form factors. We used the PDG value for $\sin\theta_C=0.2253$ [26] to obtain $|V_{cd}|=\sin\theta_C=0.2253$ and $|V_{cs}|=\cos\theta_C=0.9743$. In Fig. 3 on the left-hand-side we plot the CLEO data for both $D\to\pi$ and $D\to K$ decays. We included only the $D^0\to\pi^+(K^+)$ data. A similar study

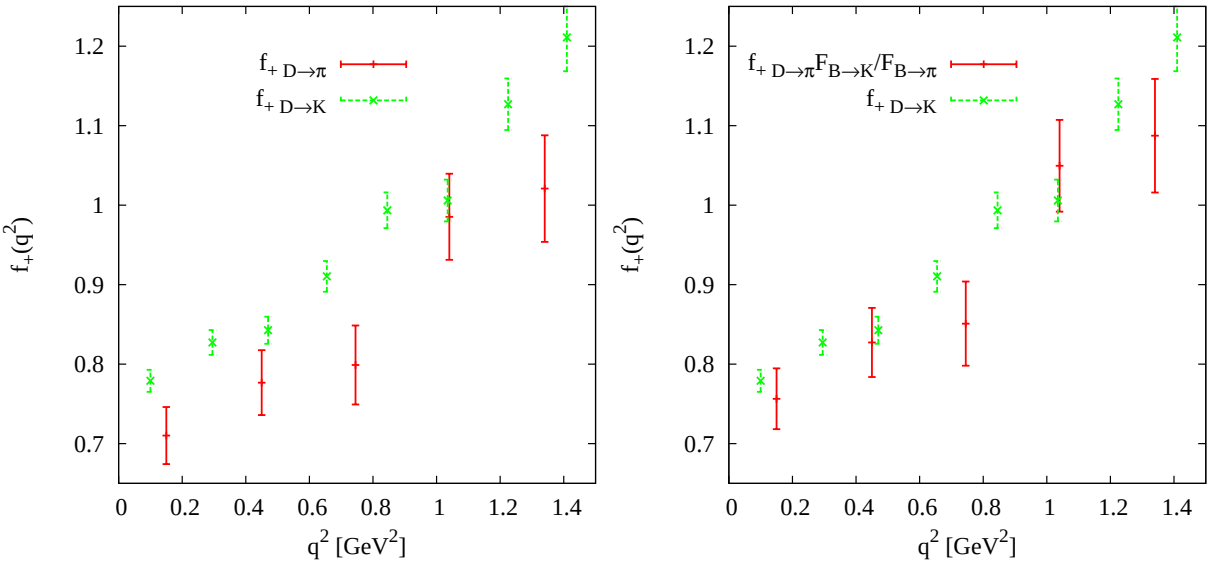

Figure 3: The measurements of CLEO [4] for the formfactor $f_+(q^2)$ for the $D \to \pi$ and the $D \to K$ semileptonic decays. In the two plots we have divided by the values of the CKM matrix elements $|V_{cd}| = 0.2253$ and $|V_{cs}| = 0.9743$ respectively. On the left we plot only the formfactors without corrections, while on the right we plot each of the two members of (37).

can be done using the $D^+ \to \pi^0(K^0)$ since they give basically the same data points as isospin symmetry dictates.

The following relation should approximately hold using (35) and the fact that the lowest order result is the same.

$$f_{+\,D\to K}(q^2) = f_{+\,D\to\pi}(q^2)\frac{F_{D\to K}}{F_{D\to\pi}}\,, \tag{37}$$

where $F_{D\to\pi(K)}$ are the logarithmic corrections due to loop diagrams quoted in (34). The corrections to relation (37) are mainly due to higher order terms i.e. $\mathcal{O}(m_M^2)$ without logarithms. We expect these corrections to be about 10%. The value of g^2, which enters through the $F_{D\to\pi(K)}$ of (37) is set to 0.44 [27]. However it does not affect the plots since the coefficients of the chiral logarithms proportional to g^2 are the same for the two decays. The scale of renormalization μ is set to $\Lambda_{\rm ChPT} \approx 1$ GeV. In the right plot of Fig. 3 the $f^+_{D\to K}$ formfactor almost overlaps the $f^+_{D\to\pi}$ one once the logarithmic corrections are taken into account as (37) indicates. By comparing the left with the right plots in Fig. 3 it is clear that our chiral logarithms compensate for the differences. Notice also that the $F_{D\to\pi(K)}$ contributes to a good 30% of the total formfactor but the total correction in the ratio is much smaller. The terms which depend on g^2 also cancel out in the ratio. (37) holds in principle both for $q^2 \ll q^2_{\rm max}$ and at the endpoint $q^2 \approx q^2_{\rm max}$. It should be kept in mind that the endpoint has quite different logarithms which are given below. The $q^2_{\rm max}$ are rather different in the two decays, being $q^2_{\rm max} \approx (1.86 - 0.49)^2 = 1.88$ GeV^2 for the K channel while $q^2_{\rm max} \approx (1.86 - 0.14)^2 = 2.9$ GeV^2 for the π channel. Therefore making a

similar comparison at large q^2 is in practice not possible. This is the reason why in Fig. 3 we stopped at $q^2 \approx 1.5$ GeV^2, the rightmost point is already rather close to the endpoint for $D \to K$.

4.4 Chiral logarithms at the endpoint

At the endpoint HPChPT is not valid but standard HMChPT is. The $B \to K$ formfactors were calculated in [24] and the $B \to \pi, K$ in [25]. The latter paper also discussed them in the partially quenched case. We do not show diagram by diagram results, these can be partly found in [24, 25]. Here we only quote the final results but we also calculate the results for the $B \to \eta$ transitions.

Again the results in this limit must give the same outcome for the two theories, since one is the relativistic limit of the other. So this is another check of the validity of our relativistic theory. Notice that we are performing a three-flavour calculation and thus there are three light masses entering into the loop-functions, i.e. m_π, m_K and m_η. This complicates the structures of the functions involved and therefore of the non-analyticities arising. For this reason a few more loop functions are also needed in the relativistic formalism compared to the two-flavour case [11]. They have been reported in the appendix. We present the results at $q^2 = q^2_{\rm max}$ for each transition using

$$f_p(q^2_{\rm max}) = f_p^{\rm Tree}(q^2_{\rm max}) F^p_{B\to M}\,, \qquad f_v(q^2_{\rm max}) = f_v^{\rm Tree}(q^2_{\rm max}) F^v_{B\to M}\,. \tag{38}$$

The relativistic theory correctly reproduces all these results provided that the substitutions $f_v^{\rm Tree}(v\cdot p) \to f_0^{\rm Tree}(q^2)$ and $f_p^{\rm Tree}(v\cdot p) \to f_+^{\rm Tree}(q^2)$ are performed.

$$\begin{aligned}
F^p_{B\to\pi} &= 1 + \left(\frac{3}{8} + \frac{43}{24}g^2\right)\frac{\overline{A}(m_\pi^2)}{F^2} + \left(\frac{1}{4} + \frac{9}{4}g^2 - \frac{m_\pi^2}{m_K^2}g^2\right)\frac{\overline{A}(m_K^2)}{F^2} \\
&\quad + \left(\frac{1}{24} + \frac{11}{24}g^2 - \frac{2}{9}\frac{m_\pi^2}{m_\eta^2}g^2\right)\frac{\overline{A}(m_\eta^2)}{F^2} + 2g^2\frac{(m_\pi^2 - m_K^2)}{F^2}\mathcal{F}\left(\frac{m_\pi}{m_K}\right) \\
&\quad + \frac{4}{9}g^2\frac{(m_\pi^2 - m_\eta^2)}{F^2}\mathcal{F}\left(\frac{m_\pi}{m_\eta}\right) \\
F^v_{B\to\pi} &= 1 + \left(\frac{11}{8} + \frac{9}{8}g^2\right)\frac{\overline{A}(m_\pi^2)}{F^2} + \left(-\frac{1}{4} + \frac{3}{4}g^2 + \frac{m_\pi^2}{m_K^2}\right)\frac{\overline{A}(m_K^2)}{F^2} \\
&\quad + \left(\frac{1}{24} + \frac{1}{8}g^2\right)\frac{\overline{A}(m_\eta^2)}{F^2} - 2\frac{m_\pi^2}{F^2}\mathcal{F}\left(\frac{m_\pi}{m_K}\right), \qquad (39) \\
F^p_{B\to K} &= 1 + \frac{9}{8}g^2\frac{\overline{A}(m_\pi^2)}{F^2} + \left(\frac{1}{2} + \frac{7}{4}g^2\right)\frac{\overline{A}(m_K^2)}{F^2} + \left(\frac{1}{6} + \frac{23}{24}g^2 - \frac{5}{9}\frac{m_K^2}{m_\eta^2}g^2\right)\frac{\overline{A}(m_\eta^2)}{F^2} \\
&\quad + \frac{10}{9}g^2\frac{(m_K^2 - m_\eta^2)}{F^2}\mathcal{F}\left(\frac{m_K}{m_\eta}\right), \\
F^v_{B\to K} &= 1 + \frac{9}{8}g^2\frac{\overline{A}(m_\pi^2)}{F^2} + \left(\frac{3}{2} + \frac{3}{4}g^2\right)\frac{\overline{A}(m_K^2)}{F^2} + \left(-\frac{1}{3} + \frac{1}{8}g^2 + \frac{m_K^2}{m_\eta^2}\right)\frac{\overline{A}(m_\eta^2)}{F^2}
\end{aligned}$$

$$
\begin{aligned}
& -2\frac{m_K^2}{F^2}\mathcal{F}\left(\frac{m_K}{m_\eta}\right), && (40)\\
F^p_{B\to\eta} &= 1+\left(\frac{3}{8}+\frac{33}{8}g^2-2\frac{m_\pi^2}{m_\eta^2}g^2\right)\frac{\overline{A}(m_\pi^2)}{F^2}+\left(\frac{1}{4}+\frac{5}{4}g^2-\frac{1}{3}\frac{m_\eta^2}{m_K^2}g^2\right)\frac{\overline{A}(m_K^2)}{F^2}\\
&\quad+\left(\frac{1}{24}+\frac{17}{72}g^2\right)\frac{\overline{A}(m_\eta^2)}{F^2}+4g^2\frac{\left(m_\eta^2-m_\pi^2\right)}{F^2}\mathcal{F}\left(\frac{m_\eta}{m_\pi}\right)\\
&\quad+\frac{2}{3}g^2\frac{\left(m_\eta^2-m_K^2\right)}{F^2}\mathcal{F}\left(\frac{m_\eta}{m_K}\right),\\
F^v_{B\to\eta} &= 1+\left(\frac{3}{8}+\frac{9}{8}g^2\right)\frac{\overline{A}(m_\pi^2)}{F^2}+\left(-\frac{5}{4}+\frac{3}{4}g^2+3\frac{m_\eta^2}{m_K^2}\right)\frac{\overline{A}(m_K^2)}{F^2}\\
&\quad+\left(\frac{1}{24}+\frac{1}{8}g^2\right)\frac{\overline{A}(m_\eta^2)}{F^2}-6\frac{m_\eta^2}{F^2}\mathcal{F}\left(\frac{m_\eta}{m_K}\right), && (41)\\
F^p_{B_s\to K} &= 1+\left(\frac{3}{8}+\frac{9}{4}g^2-\frac{3}{2}\frac{m_K^2}{m_\pi^2}g^2\right)\frac{\overline{A}(m_\pi^2)}{F^2}\\
&\quad+\left(\frac{1}{4}+2g^2\right)\frac{\overline{A}(m_K^2)}{F^2}+\left(\frac{1}{24}+\frac{7}{12}g^2-\frac{1}{18}\frac{m_K^2}{m_\eta^2}g^2\right)\frac{\overline{A}(m_\eta^2)}{F^2}\\
&\quad+3g^2\frac{(m_K^2-m_\pi^2)}{F^2}\mathcal{F}\left(\frac{m_K}{m_\pi}\right)+\frac{1}{9}\frac{(m_K^2-m_\eta^2)}{F^2}\mathcal{F}\left(\frac{m_K}{m_\eta}\right),\\
F^v_{B_s\to K} &= 1+\left(-\frac{3}{8}+\frac{3}{2}\frac{m_K^2}{m_\pi^2}\right)\frac{\overline{A}(m_\pi^2)}{F^2}+\left(\frac{3}{4}+\frac{3}{2}g^2\right)\frac{\overline{A}(m_K^2)}{F^2}\\
&\quad+\left(-\frac{5}{24}+\frac{1}{2}g^2+\frac{1}{2}\frac{m_K^2}{m_\eta^2}\right)\frac{\overline{A}(m_\eta^2)}{F^2}-3\frac{m_K^2}{F^2}\mathcal{F}\left(\frac{m_K}{m_\pi}\right)-\frac{m_K^2}{F^2}\mathcal{F}\left(\frac{m_K}{m_\eta}\right), && (42)\\
F^p_{B_s\to\eta} &= 1+\left(\frac{1}{2}+4g^2-\frac{5}{3}\frac{m_\eta^2}{m_K^2}g^2\right)\frac{\overline{A}(m_K^2)}{F^2}+\left(\frac{1}{6}+\frac{17}{18}g^2\right)\frac{\overline{A}(m_\eta^2)}{F^2}\\
&\quad+\frac{10}{3}\frac{(m_\eta^2-m_K^2)}{F^2}\mathcal{F}\left(\frac{m_\eta}{m_K}\right),\\
F^v_{B_s\to\eta} &= 1+\left(-1+\frac{3}{2}g^2+3\frac{m_K^2}{m_\pi^2}\right)\frac{\overline{A}(m_K^2)}{F^2}+\left(\frac{1}{6}+\frac{1}{2}g^2\right)\frac{\overline{A}(m_\eta^2)}{F^2}\\
&\quad-6\frac{m_\eta^2}{F^2}\mathcal{F}\left(\frac{m_\eta}{m_K}\right), && (43)
\end{aligned}
$$

with

$$
\mathcal{F}\left(\frac{m_1}{m_2}\right)=\begin{cases}-\frac{1}{(4\pi)^2}\frac{\sqrt{m_2^2-m_1^2}}{m_1}\left[\frac{\pi}{2}-\arctan\left(\frac{m_1}{\sqrt{m_2^2-m_1^2}}\right)\right] & m_1\le m_2\\ \frac{1}{(4\pi)^2}\frac{\sqrt{m_1^2-m_2^2}}{m_1}\tanh^{-1}\left(\frac{\sqrt{m_1^2-m_2^2}}{m_1}\right) & m_1\ge m_2\end{cases} \qquad (44)
$$

Our results agree with the earlier published ones in [24, 25].

5 $B \to D$ transition

5.1 Definition of formfactors

In this section we present the formalism involved in the calculation of the $B \to D$ formfactor. The matrix element for this decay is

$$\left\langle D(p') \left| \bar{b}\gamma_\mu c \right| B(p) \right\rangle \quad = \quad (p+p')_\mu \tilde{f}_+(q^2) + (p-p')_\mu \tilde{f}_-(q^2) \tag{45}$$

where q^μ is the momentum transfer $q^\mu = p - p'$.

To perform the calculation in HMChPT we need the hadronic current corresponding to the one of QCD:

$$\bar{b}\gamma_\mu c \to \mathrm{Tr}\left[X(v,v')\bar{H}(v')\gamma_\mu H(v)\right] \tag{46}$$

where v, v' are the fixed four-velocities of the B and D hadron respectively, while $X(v,v')$ is the most general bispinor constructed starting from the invariants v and v'. As explained in [20], spin symmetry for heavy quarks constrains X to be a scalar function $-\xi(v\cdot v')$, called the Isgur-Wise function [28]. The variable $v \cdot v'$ is of special importance. It can be related to q^2 through the relation

$$w \equiv v \cdot v' = \frac{m_B^2 + m_D^2 - q^2}{2 m_B m_D}\,. \tag{47}$$

The allowed kinematic range is thus $0 \le w - 1 \le \frac{(m_B - m_D)^2}{2 m_B m_D}$. w is a measure of what is the momentum transfer to the light degrees of freedom i.e. it gives us an indication of the range of applicability of HMChPT. The light degrees of freedom have momentum of order $\Lambda_{\mathrm{QCD}} v^{(\prime)}$, thus the momentum transfer to the light system is $q^2_{\mathrm{light}} \approx (\Lambda_{\mathrm{QCD}} v - \Lambda_{\mathrm{QCD}} v')^2 = 2\Lambda^2_{\mathrm{QCD}}(1-w)$. HMChPT can be applied as far as $q^2_{\mathrm{light}} \ll m^2_{b,c}$ which means on the scale $w \approx 1$ (region of zero recoil or near the endpoint) [29]. The matrix element in HMChPT is

$$\left\langle D(v') \left| \bar{b}\gamma_\mu c \right| B(v) \right\rangle_{\mathrm{HMChPT}} \quad = \quad (v+v')_\mu h_+(w). \tag{48}$$

Evaluating explicitely the trace in (46) it is easy to obtain $h_+(w) = \xi(w)$ at leading order. It can be also shown that heavy flavour symmetry implies $\xi(1) = 1$ [28, 20]. The result that one single formfactor is enough to describe the matrix element of (48) can also be achieved using the helicity formalism for counting the number of independent amplitudes [20, 30]. To compare with the results of HMChPT it is convenient to reparametrize the matrix element of QCD defined in (45) as

$$\frac{\left\langle D(p') \left| \bar{b}\gamma_\mu c \right| B(p) \right\rangle}{\sqrt{m_B m_D}} \quad = \quad (v+v')_\mu h_+(w) + (v-v')_\mu h_-(w)\,. \tag{49}$$

where the formfactors $h_\pm(w)$ are linear combinations of $\tilde{f}_\pm(q^2)$. Comparing (48) and (49) it is straightforward to see that, at leading order in $1/m_{heavy}$, $h_+(w)$ must be the same formfactor in the two formalisms and that $h_-(w) = 0$.

To perform the calculation in the relativistic framework we need the J_μ^L current responsible for the $B \to D$ transition, analogous to the one in (25). Therefore we write down all the possible independent and chiral-invariant operators that respect also heavy quark symmetries. They must contain interactions of the kind BD or B^*D^*. The first one is needed for the tree-level diagram (1) in Fig. 4, while the second for the one-loop (2) in Fig. 4. Thus the current is

$$\begin{aligned} J_\mu^L &= X_1\left(-tD^\dagger\nabla_\mu B + t\nabla_\mu D^\dagger B\right) + X_2\left(tD_\alpha^{*\dagger}\nabla_\mu B^{*\,\alpha} - t\nabla_\mu D_\alpha^{*\dagger}B^{*\,\mu}\right) \\ &\quad + X_3\left(-t\nabla^\alpha D_\alpha^{*\dagger}B_\mu^* + tD_\mu^{*\dagger}\nabla^\alpha B_\alpha^* + t\nabla^\alpha D_\mu^{*\dagger}B_\alpha^* - tD_\alpha^{*\dagger}\nabla^\alpha B_\mu^*\right) \end{aligned} \tag{50}$$

where X_1, X_2, X_3 are effective couplings and the spurion t is now a singlet under the chiral $SU(n)_L \times SU(n)_R$ symmetry since $\overline{b}\gamma_\mu c$ is a singlet. Heavy quark symmetry implies furthermore that $X_1 = X_2 = X_3$. From (50) it is easy to construct the vector current J_μ^V causing the decay.

Before concluding this section we stress once more that the zero recoil region is the only one where HMChPT is in principle applicable, as shown by [29]. This does not mean that it is not possible to extend the effective theory outside that range to calculate the infrared singularities. Indeed exactly the same arguments applied to $B \to \pi$ semileptonic decays go through for the $B \to D$ case as well, thus HPChPT can be used. As a matter of fact there have been already confirmations of how well the effective theory can do when $w - 1 \gg 0$ (see for example Fig 2.5 in [20]). The use of HPChPT justify those results.

5.2 Chiral logarithms

We now present the results for the $B_{(s)} \to D_{(s)}$ semileptonic decay. The results in two-flavour HMChPT at zero recoil ($w = 1$) can be found in [29]. The three-flavour extension has been calculated in [31] and [32]. The result at one loop and leading order in $1/m_B$ and $1/m_D$ is

$$h_+(w) = \xi(w)\left[1 + \frac{g^2}{F^2}\left(\frac{3}{2}\overline{A}(m_\pi^2) + \overline{A}(m_K^2) + \frac{1}{6}\overline{A}(m_\eta^2)\right)(r(w) - 1)\right], \tag{51}$$

and for the $B_s \to D_s$ transition it is

$$h_+(w) = \xi(w)\left[1 + \frac{g^2}{F^2}\left(2\overline{A}(m_K^2) + \frac{2}{3}\overline{A}(m_\eta^2)\right)(r(w) - 1)\right], \tag{52}$$

where

$$r(w) = \frac{1}{\sqrt{w^2 - 1}}\log\left(w + \sqrt{w^2 - 1}\right), \tag{53}$$

and $r(1) = 1$ so that the chiral logarithms cancel at zero recoil. While in [29] it has been clearly stated that the calculation is valid only at the zero recoil point, the authors of [31] and [32] present the result for the Isgur-Wise function in the whole energy range, but no explicit arguments why it should be valid are given there. The arguments of HPChPT

Figure 4: The diagrams contributing to the $B \to D$ transition up to one-loop. Notation is the same as in Fig. 1. The double lines at the left of the insertion of the current are always B mesons, while the ones in the right are D mesons.

given before imply that the formula given there are indeed valid in the whole energy regime $0 \leq w-1 \leq \frac{(m_B-m_D)^2}{2m_B m_D} \approx 1.6$. Note that here the correction is not a simple chiral logarithm as in the previous cases but there is a strong dependence on w and the result connects smoothly to the endpoint region.

We checked that our relativistic formulation gives the same result as [32]. The result up to one-loop reads

$$\begin{aligned} h_+(w) &= \frac{X_1}{\sqrt{2}}\left[1+\frac{g^2}{F^2}\left(\frac{3}{2}\overline{A}(m_\pi^2)+\overline{A}(m_K^2)+\frac{1}{6}\overline{A}(m_\eta^2)\right)\left(1-2m_B m_D \tilde{C}(m_D^2,m_B^2,q^2)\right)\right], \\ h_-(w) &= 0, \end{aligned} \tag{54}$$

where $\tilde{C}(m_D^2, m_B^2, q^2)$ comes from the three-point function $C(m^2, m_B^2, m_D^2, m_B^2, q^2, m_D^2)$ which is needed to evaluate the loop diagram in Fig. 4. In (A.15) in the appendix we define the function $\tilde{C}(m_D^2, m_B^2, q^2)$ and show that $\tilde{C}(m_D^2, m_B^2, q^2) = r(w)/(2m_B m_D)$. We also agree with the $B_s \to D_s$ result of [32].

Comparing (54) with (51) it is straightforward to see that the two formalisms give the same results as foreseen. Notice that now we do not need to distinguish the two limits $w-1 \approx 0$ and $w-1 \gg 0$: the function $r(w)$ describes the whole energy range.

Note that the reults here assume that there are no other nearby states, see e.g. the discussion in [33].

6 Conclusions

In the paper we have extended HPChPT to several processes. First we calculated the three-flavour results for the charged pion and kaon electromagnetic formfactor and the two-flavour result for the pion vector and scalar formfactor. The latter have then been used to check the underlying arguments of HPChPT in a two-loop setting.

Using the three-flavour spontaneous symmetry breaking pattern we could explicitely evaluate the dependence on the light meson masses for the $B \to \pi$ formfactors in addition to our earlier two-flavour results [11]. We could also extend the theory to other transitions as the $B \to K$ and $B \to \eta$ transitions and the corresponding B_s transitions. The corrections are of the expected size of about 30%. An unexplained feature of our results is that the two possible formfactors have always the same chiral logarithm and we ruled out two possible

explanations. A comparison with the experimental data for the $D \to \pi, K$ transition formfactors has also performed. It shows that the corrections obtained go in the right direction and are sizable. We have reproduced the known results at the endpoints and added these for the transitions to η.

Finally, we justified and reproduced already known results for the formfactors of the $B \to D$ transition at one loop.

Further investigations in this framework are desiderable, since they could significantly improve the chiral extrapolations of the lattice data. In particular it could be very useful to develop the same approach also for Partially Quenched ChPT. As stated above we expect that a formalism with an explicit power counting can be formulated along the lines of SCET.

Acknowledgments

This work is supported in part by the European Community-Research Infrastructure Integrating Activity "Study of Strongly Interacting Matter" (HadronPhysics2, Grant Agreement n. 227431) and the Swedish Research Council grants 621-2008-4074 and 621-2008-4252. This work heavily used FORM [34].

A Expansion of the needed loop integrals

We collect here the one-loop functions and their expansions, used to evaluate the diagrams in Fig. 2 and in Fig. 4 in the framework of the relativistic theory of Sect. 2.3. Much of what is written here is also present in the appendix of [11]. We need the one-, two- and three-point functions defined as ($d = 4 - 2\epsilon$)

$$A(m_1^2) = \frac{1}{i}\int \frac{d^dk}{(2\pi)^d}\frac{1}{k^2-m_1^2}, \tag{A.1}$$

$$B(m_1^2,m_2^2,p^2) = \frac{1}{i}\int \frac{d^dk}{(2\pi)^d}\frac{1}{(k^2-m_1^2)((p-k)^2-m_2^2)}, \tag{A.2}$$

$$C(m_1^2,m_2^2,m_3^2,p_1^2,p_2^2,q^2) = \frac{1}{i}\int \frac{d^dk}{(2\pi)^d}\frac{1}{(k^2-m_1^2)((k-p_1)^2-m_2^2)((k-p_1-p_2)^2-m_3^2)}, \tag{A.3}$$

with $q^2 = (p_1+p_2)^2$. Two- and three-point functions with extra powers of momenta in the numerator contribute too. They are defined similarly and the explicit definitions can be found in [35]. All these functions can be rewritten in terms of (A.1), (A.2) and (A.3) [36]. The finite parts of $A(m_1^2)$ and $B(m_1^2,m_2^2,q^2)$ are using the standard ChPT subtractions [2, 3, 37]

$$\overline{A}(m_1^2) = -\frac{m_1^2}{16\pi^2}\log\left(\frac{m_1^2}{\mu^2}\right), \tag{A.4}$$

$$\overline{B}(m_1^2,m_2^2,q^2) \;=\; \frac{1}{16\pi^2}\left[-1-\int_0^1 dx\log\left(\frac{m_1 x+m_2(1-x)-x(1-x)q^2}{\mu^2}\right)\right]. \quad (A.5)$$

As far as regards the B transitions to a light pseudoscalar meson, the three-point function $C(m_1^2,m_2^2,m_3^2,p_1^2,p_2^2,q^2)$ always depends on the masses as $(m_1^2,M^2,M^2,M^2,m_2^2,q^2)$ where m_1 is the mass of the light meson in the loop, m_2 is the mass of the light external meson and $M=m_B$. It can be rewritten using Feynman parameters x, y

$$C(m_1^2,M^2,M^2,M^2,m_2^2,q^2) = -\frac{1}{16\pi^2}\int_0^1 dx\int_0^{1-x} dy\,\times$$
$$\left[m_1^2(1-x-y)+m_2^2(-y+y^2)+M^2(x+y)^2+(q^2-M^2-m_2^2)(-y+y(x+y))\right]^{-1}. \quad (A.6)$$

In order to find the appropriate chiral logarithms we expanded (A.5) and (A.6) for small ratios m^2/M^2 . We quote only the terms of the expansions containing non-analyticities in the light masses m_i. First those only valid for $q^2 \ll q^2_{\rm max}$, i.e. away from the endpoint:

$$\overline{B}(m^2,M^2,q^2) \;=\; -\frac{1}{M^2-q^2}\overline{A}(m^2), \quad (A.7)$$

$$C(m_1^2,M^2,M^2,M^2,m_2^2,q^2) \;=\; \frac{1}{(M^2-q^2)}\frac{1}{16\pi}\frac{m_1}{M}-\frac{1}{(M^2-q^2)^2}\overline{A}(m_1^2)\,. \quad (A.8)$$

The next ones are those relevant at the endpoint or for wavefunction renormalization

$$\bar{B}(m^2,M^2,M^2) \;=\; -\frac{1}{16\pi}\frac{m}{M}+\frac{1}{16\pi}\frac{m^2}{M^2}+\frac{1}{2M^2}\overline{A}(m^2), \quad (A.9)$$

$$\bar{B}(m^2,M^2,m^2) \;=\; 0, \quad (A.10)$$

$$\bar{B}(m_1^2,M^2,(M-m_2)^2) \;=\; \frac{1}{M}\left[2m_2\mathcal{F}\left(\frac{m_1}{m_2}\right)-\frac{m_2}{m_1^2}\overline{A}(m_1^2)\right]$$
$$+\frac{1}{M^2}\left[3m_2^2\mathcal{F}\left(\frac{m_1}{m_2}\right)+\overline{A}(m_1^2)\left(\frac{1}{2}-\frac{3}{2}\frac{m_2^2}{m_1^2}\right)\right]. \quad (A.11)$$

The function $\mathcal{F}(m_1/m_2)$ was defined in (44). The expansion in (A.11) holds in both the cases $m_2 \lesseqgtr m_1$ and also for $m_1=m_2$ where it correctly reduces to the expansion reported in the appendix of [11].

The expansions of the three-point functions at $q^2_{\rm max}$ are a bit more involved. The reason is that the reduction formulas present a singularity at $q^2_{\rm max}=(M-m_2)^2$ for $m_2^2=0$. Furthermore we need to distinguish different cases depending on the m_1 and m_2 appearing in the arguments of the three-loop functions. We use again the same technique used in [11]. We expand each of the functions directly from the Feynman parameter integral, without first rewriting them in terms of (A.1), (A.2) and (A.3). To do this one rewrites the integral in (A.6) using $z=x+y$ as

$$C(m_1^2,M^2,M^2,M^2,m_2^2,(M-m_2)^2) = -\frac{1}{16\pi^2}\int_0^1 dz\int_0^z dy\times$$
$$\frac{1}{[M^2z^2+m_1^2+2m_2My+(-m_1^2z+m_2^2(-y+y^2)-2m_2Myz)]}. \quad (A.12)$$

The part in the denominator in brackets is always suppressed by at least m/M compared to the first three terms for all values of z and y and we can thus expand in it. The remaining integrals can be done with elementary means. The expansions obtained are many and long, therefore we quote only those needed and restricted to those terms where a infrared singularity appears. We do not quote terms like $1/(4\pi)^2 m/M^3$, also non-analytic for small m, because they always cancel in the final results (39)-(43). The expansions read

$$
\begin{aligned}
C(m_1^2,M^2,M^2,M^2,m_2^2,(M-m_2)^2) &= \frac{1}{M^2}\left[-\frac{1}{2}\frac{1}{m_1^2}\overline{A}(m_1^2)+\mathcal{F}\left(\frac{m_1}{m_2}\right)\right] \\
&+\frac{1}{M^3}\left[\mathcal{F}\left(\frac{m_1}{m_2}\right)m_2-\frac{1}{2}\frac{m_2}{m_1^2}\overline{A}(m_1^2)\right]+\frac{1}{M^4}\left[-\frac{1}{2}\frac{m_2^2}{m_1^2}\overline{A}(m_1^2)+\mathcal{F}\left(\frac{m_1}{m_2}\right)\left(m_2^2+\frac{3}{8}m_1^2\right)\right], \\
C_{11}(m_1^2,M^2,M^2,M^2,m_2^2,(M-m_2)^2) &= \frac{1}{M^3}\left(-\mathcal{F}\left(\frac{m_1}{m_2}\right)m_2+\frac{1}{2}\frac{m_2}{m_1^2}\overline{A}(m_1^2)\right) \\
&+\frac{1}{M^4}\left[\left(-\frac{1}{2}+\frac{13}{12}\frac{m_2^2}{m_1^2}\right)\overline{A}(m_1^2)-\mathcal{F}\left(\frac{m_1}{m_2}\right)\left(\frac{13}{6}m_2^2-\frac{1}{6}m_1^2\right)\right], \\
C_{12}(m_1^2,M^2,M^2,M^2,m_2^2,(M-m_2)^2) &= \frac{1}{M^3}\left(-\mathcal{F}\left(\frac{m_1}{m_2}\right)\left(\frac{2}{3}m_2+\frac{1}{3}\frac{m_1^2}{m_2}\right)+\frac{1}{3}\frac{m_2}{m_1^2}\overline{A}(m_1)\right) \\
&+\frac{1}{M^4}\left[\left(-\frac{1}{4}+\frac{5}{6}\frac{m_2^2}{m_1^2}\right)\overline{A}(m_1^2)-\mathcal{F}\left(\frac{m_1}{m_2}\right)\left(\frac{5}{3}m_2^2+\frac{1}{3}m_1^2\right)\right], \\
C_{21}(m_1^2,M^2,M^2,M^2,m_2^2,(M-m_2)^2) &= \frac{1}{M^4}\left[-\mathcal{F}\left(\frac{m_1}{m_2}\right)\left(-\frac{4}{3}m_2^2+\frac{1}{3}m_1^2\right)\right. \\
&\left.+\overline{A}(m_1^2)\left(\frac{1}{2}-\frac{2}{3}\frac{m_2^2}{m_1^2}\right)\right], \\
C_{22}(m_1^2,M^2,M^2,M^2,m_2^2,(M-m_2)^2) &= \frac{1}{M^4}\left[\mathcal{F}\left(\frac{m_1}{m_2}\right)\left(\frac{4}{5}m_2^2+\frac{1}{15}m_1^2+\frac{2}{15}\frac{m_1^4}{m_2^2}\right)\right. \\
&\left.+\overline{A}(m_1^2)\left(\frac{1}{6}-\frac{2}{5}\frac{m_2^2}{m_1^2}\right)\right], \\
C_{23}(m_1^2,M^2,M^2,M^2,m_2^2,(M-m_2)^2) &= \frac{1}{M^4}\left[\mathcal{F}\left(\frac{m_1}{m_2}\right)m_2^2+\overline{A}(m_1^2)\left(\frac{1}{4}-\frac{1}{2}\frac{m_2^2}{m_1^2}\right)\right], \\
C_{24}(m_1^2,M^2,M^2,M^2,m_2^2,(M-m_2)^2) &= \frac{1}{M^2}\left[-\mathcal{F}\left(\frac{m_1}{m_2}\right)\frac{1}{3}(m_2^2-m_1^2)\right. \\
&\left.+\overline{A}(m_1)\left(-\frac{1}{4}+\frac{1}{6}\frac{m_2^2}{m_1^2}\right)\right]. \qquad \text{(A.13)}
\end{aligned}
$$

Setting the masses $m_1 = m_2$ all the expansions in (A.13) coincide correctly with the ones reported in the appendix of [11]. The function $\mathcal{F}(m_1/m_2)$ is the one defined in (44). Notice that it takes different forms depending if $m_1 \lesseqgtr m_2$. Furthermore for $m_1 = m_2$ $\mathcal{F}(m_1/m_2) = 0$. The other three-point functions do not give any leading contribution.

We focus now on the semileptonic decay $B \to D$. The three-point function entering in the loop diagram of Fig. 4 is $C(m^2, M_1^2, M_2^2, M_1^2, q^2, M_2^2)$, where m is the mass of the light

meson in the loop, $M_1 = m_B$ and $M_2 = m_D$. To expand it, similarly to what has been done above, we first rewrite it in terms of the Feynman parameters x, y

$$C(m^2, M_1^2, M_2^2, M_1^2, q^2, M_2^2) = -\frac{1}{16\pi^2}\int_0^1 dx \int_0^{1-x} dy \times \\ \left[m^2(1-x-y) + x^2 M_1^2 + y^2 M_2^2 + xy(M_1^2 + M_2^2 - q^2)\right]^{-1} . \qquad (A.14)$$

The $m^2(x+y)$ term in (A.14) is suppressed by at least one power of m so we can neglect it. Setting $x = X/M_1$, $y = Y/M_2$ and $w = (M_1^2 + M_2^2 - q^2)/(2M_1M_2)$ the integral becomes

$$C(m^2, M_1^2, M_2^2, M_1^2, q^2, M_2^2) = -\frac{1}{16\pi^2}\frac{1}{M_1 M_2}\int_0^{M_1} dX \int_0^{M_2 - \frac{M_2}{M_1}X} dY \left[m^2 + X^2 + Y^2 + 2wXY\right]^{-1} .$$

Then we can perform another change of variable and set polar coordinates $X = R\cos\phi$, $Y = R\sin\phi$:

$$C(m^2, M_1^2, M_2^2, M_1^2, q^2, M_2^2) = -\frac{1}{16\pi^2}\frac{1}{M_1 M_2}\int_0^{\pi/2} d\phi \int_0^{R_{\max}} dR R \left[m^2 + R^2 + 2wR^2\sin(2\phi)\right]^{-1} ,$$

where the upper boundary is $R_{\max} = M_2/(\sin\phi + M_2/M_1\cos\phi)$. We are interested in isolating the infrared singularities. Those only arise from the lower bound of the integral. Therefore, performing the integral in dR, we keep only the term coming from the small R region. However we checked explicitely that the large R region does not produce any soft singularity at the desired order. The result for the integral in R reads

$$C(m^2, M_1^2, M_2^2, M_1^2, q^2, M_2^2) = \frac{1}{16\pi^2}\frac{1}{2M_1 M_2}\int_0^{\pi/2} d\phi \log\left(\frac{m^2}{\mu^2}\right)\left[1 + 2w\sin(2\phi)\right]^{-1} + \cdots ,$$

where the ellipsis are the terms coming from the upper bound and μ is a parameter with the dimension of a mass. The integral in $d\phi$ can be done analitycally and after tedious calculations we arrive to the final result

$$\begin{aligned} C(m^2, M_1^2, M_2^2, M_1^2, q^2, M_2^2) &= \frac{1}{16\pi^2}\frac{1}{2M_1 M_2}\frac{1}{\sqrt{w^2-1}}\log\left(w + \sqrt{w^2-1}\right)\log\left(\frac{m^2}{\mu}\right) + \ldots \\ &= \frac{1}{16\pi^2}\tilde{C}(M_2^2, M_1^2, q^2)\log\left(\frac{m^2}{\mu^2}\right) + \ldots . \qquad (A.15) \end{aligned}$$

References

[1] S. Weinberg, Physica **A96** (1979) 327.

[2] J. Gasser and H. Leutwyler, Annals Phys. **158** (1984) 142.

[3] J. Gasser and H. Leutwyler, Nucl. Phys. B **250** (1985) 465.

[4] J. Y. Ge *et al.* [CLEO Collaboration], Phys. Rev. D **79** (2009) 052010 [arXiv:0810.3878 [hep-ex]].

[5] N. E. Adam *et al.* [CLEO Collaboration], Phys. Rev. Lett. **99** (2007) 041802 [arXiv:hep-ex/0703041].

[6] T. Hokuue *et al.* [Belle Collaboration], Phys. Lett. B **648** (2007) 139 [arXiv:hep-ex/0604024].

[7] B. Aubert *et al.* [BABAR Collaboration], Phys. Rev. Lett. **98** (2007) 091801 [arXiv:hep-ex/0612020].

[8] E. Gamiz, PoS **LATTICE2008** (2008) 014 [arXiv:0811.4146 [hep-lat]], and references therein.

[9] J. M. Flynn and C. T. Sachrajda [RBC Collaboration and UKQCD Collaboration], Nucl. Phys. B **812** (2009) 64 [arXiv:0809.1229 [hep-ph]].

[10] J. Bijnens and A. Celis, Phys. Lett. B **680** (2009) 466 [arXiv:0906.0302 [hep-ph]].

[11] J. Bijnens and I. Jemos, Nucl. Phys. B **840** (2010) 54 [arXiv:1006.1197 [hep-ph]], Erratum Nucl. Phys. B **844** (2011) 182

[12] J. Bijnens, G. Colangelo and P. Talavera, JHEP **9805** (1998) 014 [arXiv:hep-ph/9805389].

[13] J. Bijnens, G. Colangelo and G. Ecker, JHEP **9902** (1999) 020 [arXiv:hep-ph/9902437].

[14] A. Pich, Lectures at Les Houches Summer School in Theoretical Physics, Session 68: Probing the Standard Model of Particle Interactions, Les Houches, France, 28 Jul - 5 Sep 1997, [hep-ph/9806303].

[15] S. Scherer, *Adv. Nucl. Phys.*, 27 (2002) 277 [hep-ph/0210398].

[16] M. B. Wise, Phys. Rev. D **45** (1992) 2188.

[17] G. Burdman and J. F. Donoghue, Phys. Lett. B **280** (1992) 287.

[18] J. L. Goity, Phys. Rev. D **46** (1992) 3929 [arXiv:hep-ph/9206230].

[19] M. B. Wise, Lectures given at CCAST Symp. on Particle Physics at the Fermi scale, arXiv:hep-ph/9306277.

[20] A. V. Manohar and M. B. Wise, Camb. Monogr. Part. Phys. Nucl. Phys. Cosmol. **10** (2000) 1.

[21] S. Fleming, PoS(EFT09)002 [arXiv:0907.3897 [hep-ph]], and references therein.

[22] J. Gasser and H. Leutwyler, Nucl. Phys. B **250** (1985) 517.

[23] J. Bijnens, F. Cornet, Nucl. Phys. **B296** (1988) 557.

[24] A. F. Falk and B. Grinstein, Nucl. Phys. B **416** (1994) 771 [arXiv:hep-ph/9306310].

[25] D. Becirevic, S. Prelovsek and J. Zupan, Phys. Rev. D **68** (2003) 074003 [arXiv:hep-lat/0305001].

[26] KNakamura *et al.* [Particle Data Group Collaboration], J. Phys. G **G37** (2010) 075021.

[27] G. M. de Divitiis, L. Del Debbio, M. Di Pierro, J. M. Flynn, C. Michael and J. Peisa [UKQCD Collaboration], JHEP **9810** (1998) 010 [arXiv:hep-lat/9807032].

[28] N. Isgur, M. B. Wise, Phys. Lett. **B237** (1990) 527.

[29] L. Randall, M. B. Wise, Phys. Lett. **B303** (1993) 135-139. [hep-ph/9212315].

[30] H. D. Politzer, Phys. Lett. B **250** (1990) 128.

[31] E. E. Jenkins, M. J. Savage, Phys. Lett. **B281** (1992) 331-335.

[32] C. G. Boyd, B. Grinstein, Nucl. Phys. **B451** (1995) 177-193. [hep-ph/9502311].

[33] J. O. Eeg, S. Fajfer, J. F. Kamenik, JHEP **0707** (2007) 078. [arXiv:0705.4567 [hep-ph]].

[34] J. A. M. Vermaseren, arXiv:math-ph/0010025.

[35] J. Bijnens and P. Talavera, JHEP **0203** (2002) 046 [arXiv:hep-ph/0203049].

[36] G. Passarino and M. J. G. Veltman, Nucl. Phys. B **160** (1979) 151.

[37] G. 't Hooft and M. J. G. Veltman, Nucl. Phys. B **153** (1979) 365.